PRESS FORMING OF E-GLASS FABRIC REINFORCED POLYPROPYLENE: A NUMERICAL STUDY

Chandra Kishore Reddy Emani, P. K. Mallick
Department of Mechanical Engineering, University of Michigan-Dearborn, MI 48128

Abstract

This study focuses on numerically analyzing the deformation behavior of E-glass fabric reinforced polypropylene (PP) prepreg during press forming. A finite element modeling technique is employed in which membrane and shell elements are superimposed to accurately simulate both in-plane and out-of-plane deformations of woven fabrics under shear loading, while also considering the deformation characteristics of the matrix material. The model is capable of predicting the maximum draw depths achieved just before failure for the fabric-reinforced PP. The proposed approach represents the prepreg sheet as a superimposed layer consisting of PP and fabric. Under-integrated membrane elements are used to capture the in-plane shear deformation of the fabric, while fully integrated shell elements are used to account for the out-of-plane bending behavior of the fabric and the deformation of the matrix material during press forming.

Press forming simulations were conducted with various initial blank temperatures. The draw depths achieved by the prepreg before failure were compared to those achieved with a single layer of unfilled PP using the identical die-punch setup. Failure in the prepreg occurred in the PP layer, where the plastic strains surpassed the failure strain of polypropylene. The highest shear deformation was observed along the diagonal at the die entry radius, coinciding with the location of failure in the PP layer. Additionally, the fabric layer displayed a tendency to buckle after failure initiation in the PP layer.

Keywords: dry fabric, fabric-reinforced PP, press forming, shear deformation, buckling, draw depth

1. INTRODUCTION

Fabric-reinforced composites are finding increasing number of applications in automotive body panels and structures, such as roof panel and B-pillars. They are also widely used in other industries, such as aerospace, construction and sports. The reasons for their increasing use are their high fracture toughness, damage tolerance, ability to maintain structural integrity, and handleability during manufacturing of composite parts. The manufacturing process for making fabric reinforced composite automotive parts using a thermosetting resin is called liquid composite molding (LCM) that involves the injection of a liquid resin into a dry fabric preform and curing the resin in place [1]. If a thermoplastic polymer is selected as the matrix material, then the fabric is first embedded in the matrix to form a prepreg, which is followed by a press forming operation to make the composite part [1]. Out of these two manufacturing methods, press forming has lower cycle times compared to LCM and can be easily adapted in the automotive industry with a few modifications to the metal forming dies

that are used with sheet metals. One of the modifications is the addition of heating elements, since the press forming operation must be performed at elevated temperatures for the prepreg to deform adequately to conform to the die shape and form a defect-free part.

Depending on the press forming conditions used, fabric deformation characteristics, and the die-punch design, several defects may form in the fabric. They include fiber distortion, wrinkles and tearing. Most of the deformation characteristic studies on press forming of fabric reinforced thermoplastic polymers are mainly focused on the influence of the shear properties of the fabric and neglect the effect of the influence of the matrix material [2, 3]. Also, the press forming simulations are usually carried out at or above melting temperature of the matrix material, with the assumption that the matrix material is in a liquid state and offer little resistance to the deformation of the fabric, and hence the effect of the matrix material is ignored.

In the current work, deep drawing of E-glass fabric reinforced polypropylene (PP) was studied using LS-Dyna, a commercially available and widely used finite element software for nonlinear analysis of structures and processes. In this study, the processing window was selected to be between 25 and 150°C, which is below the melting point of polypropylene homopolymer [4]. For the temperatures under consideration, the influence of the matrix material during press forming cannot be ignored. Since during press forming the matrix is in a soft solid state, its influence must be incorporated to determine the true deformation behavior of the E-glass fabric reinforced PP.

Several studies have examined the impact of matrix materials in press forming processes. Tabiei and Murugesan [5] employed the PART_COMPOSITE control card in LS-Dyna and represented the prepreg using a single layer of shell elements with varying integration points throughout the thickness. Chen et al. [6] utilized a solid-shell element approach to model thermoplastic composites. Wang et al. [7] proposed a simulation methodology for thermoforming multilayer composites, employing semi-discrete shell elements to represent each layer. In an extension of the previously proposed macro-scale model approach for dry fabrics, Nishi et al. [8] incorporated additional shell elements surrounding the textile membrane to account for fabric deformation [9] and consider the effects of the thermoplastic resin. Out of the various methods mentioned, only the method proposed by Tabiei et al. [5] and Nishi et al. [8] take into account the effect of the blank temperature during press forming. However, the method by Tabiei et al. [5] does not differentiate the failure modes, i.e., it cannot predict if the failure has occurred in the matrix material or in the fabric. Hence, this calls for the need for a new methodology that can predict the deformation characteristics of the prepreg and also take into account the effect of the blank temperature and identify the failure modes.

A simulation methodology using the superimposed approach is developed in this study to understand the deformation behavior of fabric-reinforced PP prepreg during press forming operation and predict the draw depths that can be attained at different blank temperatures without failure. The superimposed method assumes that the prepreg sheet contains the fabric embedded in the polypropylene matrix. The total force required for

press forming the prepreg sheet will be additive in nature of the force required to deform the fabric and the force required to deform the matrix material. The draw depths attained before failure in press forming of the prepreg at different temperatures are determined and compared with the draw depths attained in press forming a single sheet of unfilled polypropylene of equivalent thickness. The type of failure, failure location and the reason for the failure for both fabric-reinforced matrix material and single layer of material are identified in this study.

2. MATERIAL CHARACTERIZATION

The thermoplastic prepreg under consideration in this study is an E-glass fiber reinforced polypropylene homopolymer. The tensile stress-strain relationship of the unfilled polypropylene (PP) is defined by the following three-parameter nonlinear constitutive model proposed by Zhou and Mallick [10].

$$\sigma = \frac{E(\dot{\varepsilon}, T)\,\varepsilon}{1 + E(\dot{\varepsilon}, T)\,\beta(\dot{\varepsilon}, T)\,\varepsilon^{m}} \qquad (1)$$

In Equation (1), the stress σ is expressed as a function of strain ε, modulus E, and compliance factor β and strain exponent m. Both E and β depend on the strain rate $\dot{\varepsilon}$ and the temperature T, but m is considered a constant. To account for the effects of varying temperature and strain rate on the modulus, yield strength and compliance factor of PP, a parametric equation of the general form shown in Equation (2) was used. The details about the constants a, b and c, reference temperature T_o and reference strain rate $\dot{\varepsilon}_0$ can be found in Ref. [11].

$$E, \sigma_y, \beta = a\left(1 + b \cdot \ln\left(\frac{\dot{\varepsilon}}{\dot{\varepsilon}_0}\right)\right) \cdot exp\left(c.\left(T - T_0\right)\right) \qquad (2)$$

The values of the modulus, yield strength and compliance factor at different temperatures and strain rates were obtained using Equation 2, which were then substituted in Equation 1 to obtain a series of tensile stress-strain curves of PP at different temperatures and strain rates, an example of which is shown in Figure 1 at a strain rate of 0.1 s^{-1}. The theoretical stress-strain curves thus generated were given as an input for finite element simulations to simulate the behavior of matrix material. During press forming with blank at elevated initial temperatures, the temperature of the blank can decrease as it comes in contact with the die and the punch that are maintained at room temperature due to the conduction heat transfer. The decrease in temperature of the blank alters the properties of the PP at different sections of the blank which in turn affects the drawability of both PP and E-glass fabric reinforced PP. Hence, to determine the true behavior for single PP layer and E-glass fabric reinforced PP, the variation of yield strength, modulus and failure strain with temperature were also given as an input for finite element simulations, details of which can be found in Ref. [11].

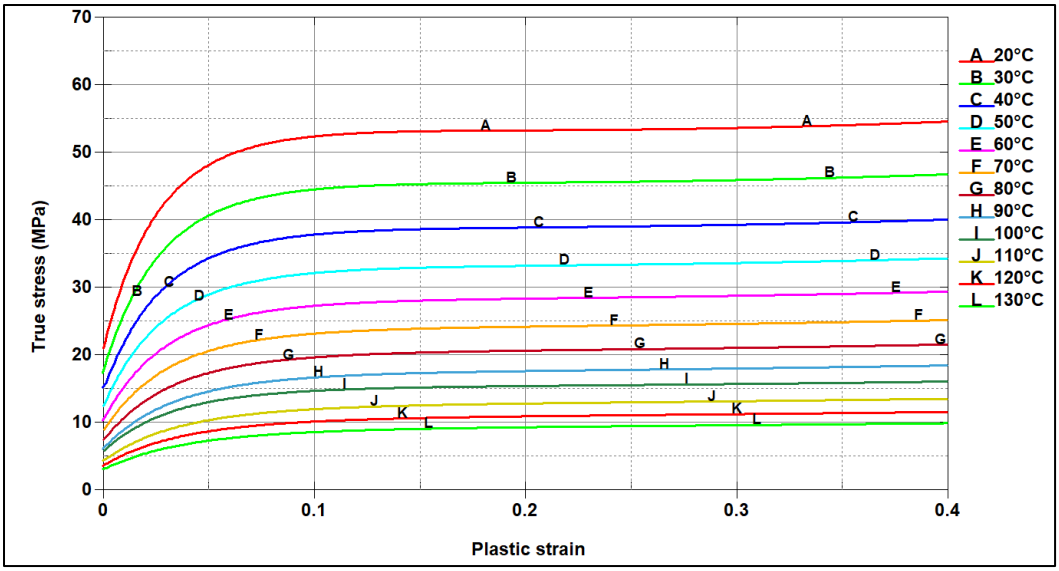

Figure 1: Stress-strain curves at 0.1 s^{-1} and different temperatures ranging from 20 to 130˚C.

Three different plain-weave bidirectional E-glass fabrics were used as the reinforcement material. Their physical characteristics as listed by the supplier, Fibre Glast Development Corp., and obtained by image analysis are provided in Table 1. Different material parameters to simulate the behavior of E-glass fabrics can be found in Ref. [12].

Table 1: Physical characteristics of plain-weave E-glass fabrics used in the study [13].

Fabric Style	Fabric Weight	Fabric Thickness	Warp and Weft (Fill) Counts	Yarn Description
1610 (2 oz fabric)	2.38 oz/yd^2 (80 g/m^2)	0.004 in (0.1 mm)	32/in and 28/in (12.59/cm and 11.02/cm)	ECG 150 1/0 (US) EC9 33 (SI)
1522 (4 oz fabric)	3.67 oz/yd^2 (124 g/m^2)	0.006 in (0.15 mm)	24/in and 22/in (9.4/cm and 8.7/cm)	ECG 150 1/2 (US) EC9 33 x 2 (SI)
3733 (6 oz fabric)	5.8 oz/yd.^{2} (197 g/m^2)	0.007 in (0.2 mm)	18/in and 18/in (7.09/cm and 7.09/cm)	ECG 37 1/0 EC9 134 (SI)

3. PRESS FORMING SETUP AND FINITE ELEMENT MODEL

Figure 2 shows the press forming setup and the finite element model used for studying the deep drawability of E-glass fabric reinforced polypropylene. It consists of an open round die of 80 mm diameter and 10 mm corner radius, a flat round blank holder, and a punch of 76 mm diameter with two different corner radii, namely 15 mm and 8 mm. The dimensions of the die and the punch were selected to keep the radial gap between the die wall and the punch at 2 mm. The punch velocity was 100 mm/s. A blank holder force of 800 N was applied on

the blank to avoid wrinkle formation at very low draw depths due to yarn buckling at the intersection of the flanges, as was observed in press forming experiments with dry fabrics at lower blank holder forces [14]. A square prepreg sheet, measuring 160 mm x 160 mm in aerial dimensions, was used as the blank. The total thickness of the fabric-reinforced PP blank was considered to be 1 mm.

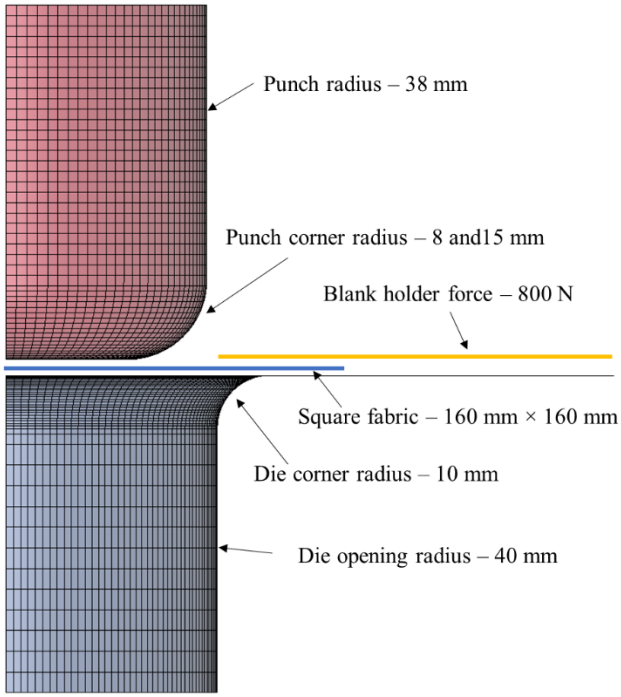

Figure 2: Finite element model of the quarter of the press forming setup.

To conduct the finite element simulation, it was assumed that the fabric-reinforced polypropylene prepreg behaves as a fabric layer embedded in a PP matrix layer (Figure 3). Because of symmetry conditions and to reduce the computational time, only a quarter model was used for which the blank size was 80 mm x 80 mm, and the blank holder force was 200 N. The mesh size for the die and the punch was selected to be 2 mm; however, a higher mesh density at both punch and die corner radii was used to accommodate the geometrical inconsistencies during press forming. A mesh size of 1.5 mm was chosen for the quadrilateral elements in the fabric and matrix layers. These layers are overlaid, and any duplicate nodes resulting from this superimposition are merged together so that they are mutually constrained and share the same nodes.

The die material was selected to be aluminum and was modeled using MAT_020 (MAT_RIGID). Three regions of contact of the die-punch material with fabric-reinforced PP and unfilled PP were considered in the FE simulations: (1) contact between the punch and the blank, (2) contact between the blank holder and the blank, and (3) contact between the die wall and the blank. The friction coefficients at the regions of contact were taken from the study by Chung et al. [15]. The friction values given as an input for the FE simulations are based on the assumption that the majority of PP is in contact with the dies and the friction conditions are

controlled by the matrix material with neglecting the influence of the fabric material. These values were selected based on the initial temperature of the blank and were assigned a constant value.

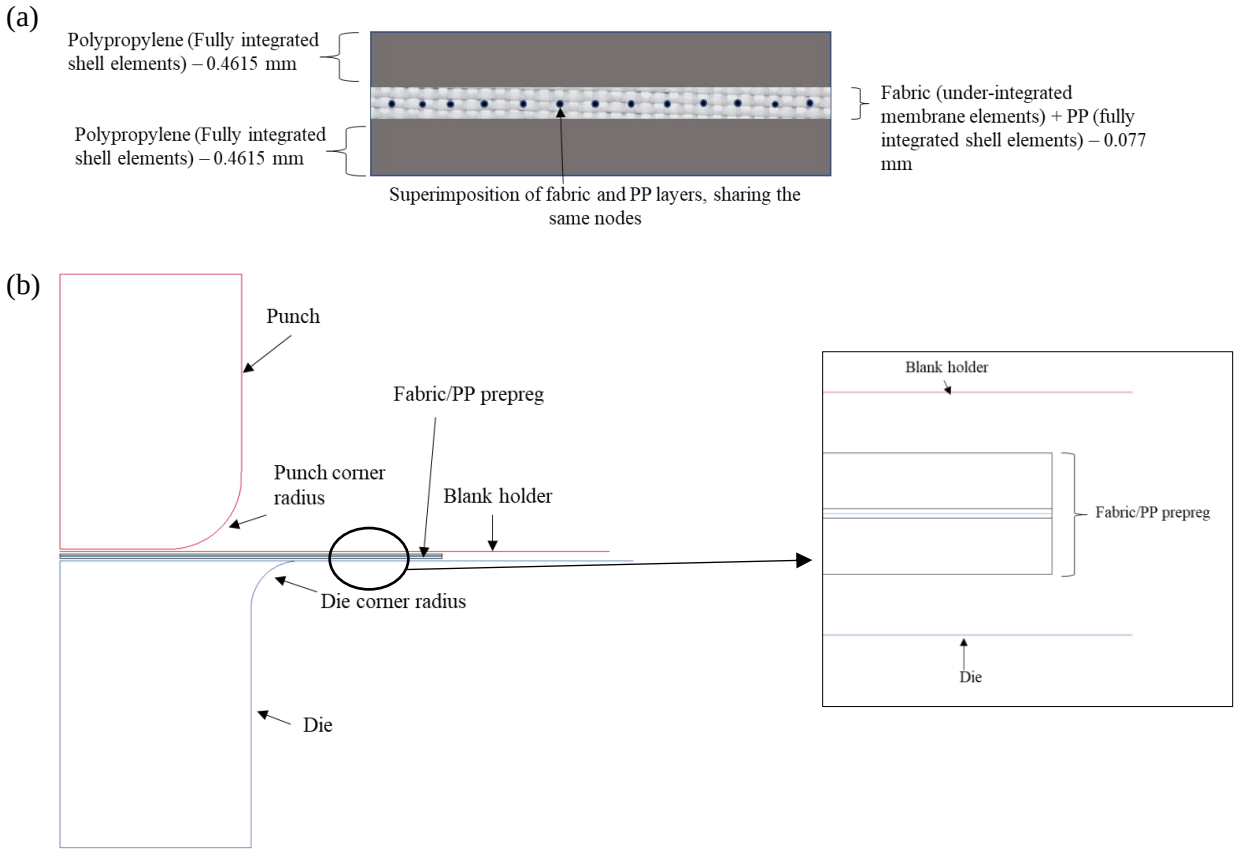

Figure 3: (a) Superimposed model representing fabric/PP prepreg, (b) schematic representation of the press forming setup for fabric/PP prepreg.

Since the forming speed was 100 mm/s and temperature variation during forming was expected to be very small, all numerical studies were carried out at isothermal conditions so that the temperature of the fabric-reinforced PP blank and the unfilled PP blank remained constant and there was no heat loss due to thermal conduction from the blank to the die or the punch. The thermal properties of the dies, PP, and E-glass fibers are listed in Table 2. However, it should be noted that the superimposed approach presented in this study can capture the deformation of fabric reinforced PP under non-isothermal conditions where it can take into consideration the variation of temperature of the blank with time.

Table 2: Thermal properties of aluminum and PP.

Parameter	Aluminum [16]	Polypropylene [17]	E-glass fibers [18]
Heat Capacity (J/kg. K)	900	1800	810
Thermal conductivity (W/m. K)	205	0.14	0.05

4. MATERIAL MODELS AND MODELING APPROACH

Out of the several different material models available in LS-Dyna to simulate fabric deformation, MAT_234 (MAT_VISCOELASTIC_LOOSE_FABRIC) was selected in this study since it gives a more stable shear angle distribution compared to MAT_235 (Micromechanics dry fabric model) and MAT_249 (Anisotropic hyper-elastic model), and also the outer contour/ shape profile of the press formed fabric matches well with the experimental shape [19]. MAT_234 exclusively supports membrane elements and cannot be utilized with shell elements. This limitation stems from the relatively lower flexural stiffness of fabrics in comparison to their tensile stiffness, making them prone to buckling under in-plane compression. To simplify the numerical determination of the behavior of fabrics, it is common practice to disregards bending stiffness and use membrane assumption [20]. MAT_234 assigned to fully integrated membrane elements exhibits tension locking phenomenon, in which the predicted forces required for the fabric deformation are higher than that observed in the experimental conditions [21]. However, if MAT_234 is assigned to the under-integrated membrane elements to avoid tension locking phenomenon [21], multiple small wrinkles are formed which are not observed experimentally [9, 22]. The reason for the multiple small wrinkles can be attributed to the membrane elements not being able to include out-of-plane bending stiffness. Different modeling approaches have been proposed [9, 23, 24, 25, 26] that include in-plane shear behavior and out-of-plane bending stiffness for the dry fabrics so that they represent the true fabric deformation. Studies have shown that the superimposed approach [26] in which the shell and membrane elements are superimposed on one another with MAT_234 assigned to the membrane elements and isotropic elastic material model MAT_001 assigned to the shell elements [27] with a very small tensile modulus (determined from the flexural rigidity of the fabric material or obtained by trial and error method to match the uniaxial bias-extension simulations with the experimental results) can replicate the experimental results. The value of the modulus that is to be assigned to the shell elements is very low, usually less than 0.001% of the modulus of the fabric and such a low value will not affect the in-plane shear properties of the fabric. The effectiveness of the superimposed approach is demonstrated in Figures 4 and 5 where the experimental outer shape profile of the Fabric_1610 and the punch force vs. punch displacement graphs are compared with simulated results. From these figures, it can be seen that the simulation based on the superimposed approach is able to closely replicate the fabric deformation behavior observed experimentally.

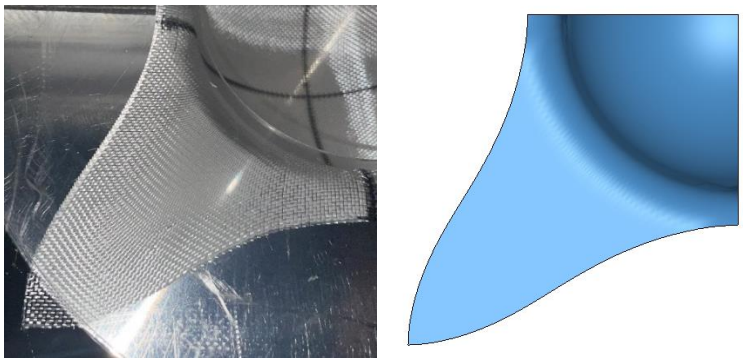

Figure 4: Comparison of experimental outer shape profile (left) and simulated outer shape profile (right) at the end of press forming of a dry E-glass fabric (Fabric_ 1610).

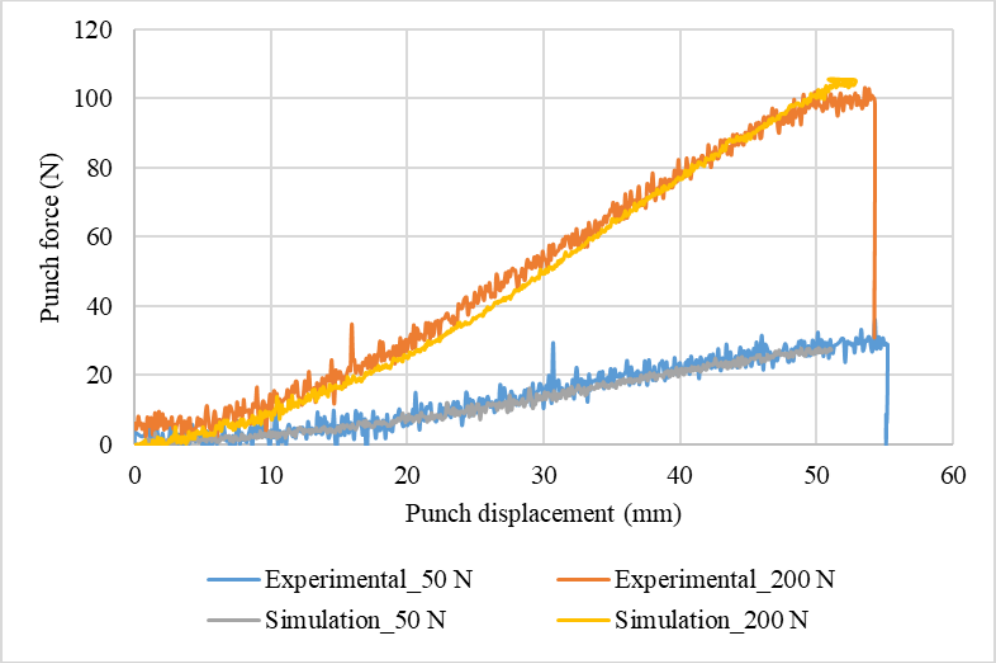

Figure 5: Comparison of experimental and simulated punch force vs. punch displacement graphs for Fabric_1610 (2 oz) at two different blank holder forces (50 N and 200 N) with 38 mm punch corner radius.

The concept of superimposition of shell and membrane elements for simulating dry fabrics was carried forward to simulate the deformation behavior of fabric-reinforced PP during the press forming operation. The modeling approach for fabric-reinforced PP involves the superimposition of shell and membrane elements on one another. In this study, the fabric-reinforced PP is a 1-mm thick prepreg sheet of a 0.077 mm fabric layer embedded in the PP matrix of 1 mm thickness (Figure 3). The concept of the superimposed approach for the dry fabrics and the fabric-reinforced polymer is shown in Figure 6. The fabric was represented by membrane elements, which effectively captured the in-plane shear deformation of the fabric, whereas polypropylene was modeled using shell elements, which accounted for both the deformation characteristics of the matrix material and the out-of-plane bending behavior of the embedded fabric. The fabric and PP layers were superimposed on

one another and the duplicate nodes arising due to superimposition were merged into single common nodes to represent a fabric-reinforced PP prepreg. By merging the duplicate nodes, the fabric and matrix layers become mutually constrained, allowing them to share the same nodes and deform together during the analysis. This approach enables the simulation to accurately capture the interaction and behavior of the fabric and matrix layers as a composite material system. The under-integrated membrane elements were assigned to the fabric using MAT_234 and the fully integrated shell elements were assigned to the PP layers using MAT_106 (to take into account the effects of the varying temperature and strain rate). The total stress obtained during the deformation is the sum of the stress required for forming of fabric material and the stress for press forming of PP layers. During press forming of E-glass fabric reinforced PP, there can be additional stresses introduced in the matrix layers due to the shear locking tendency exhibited by the fabric material.

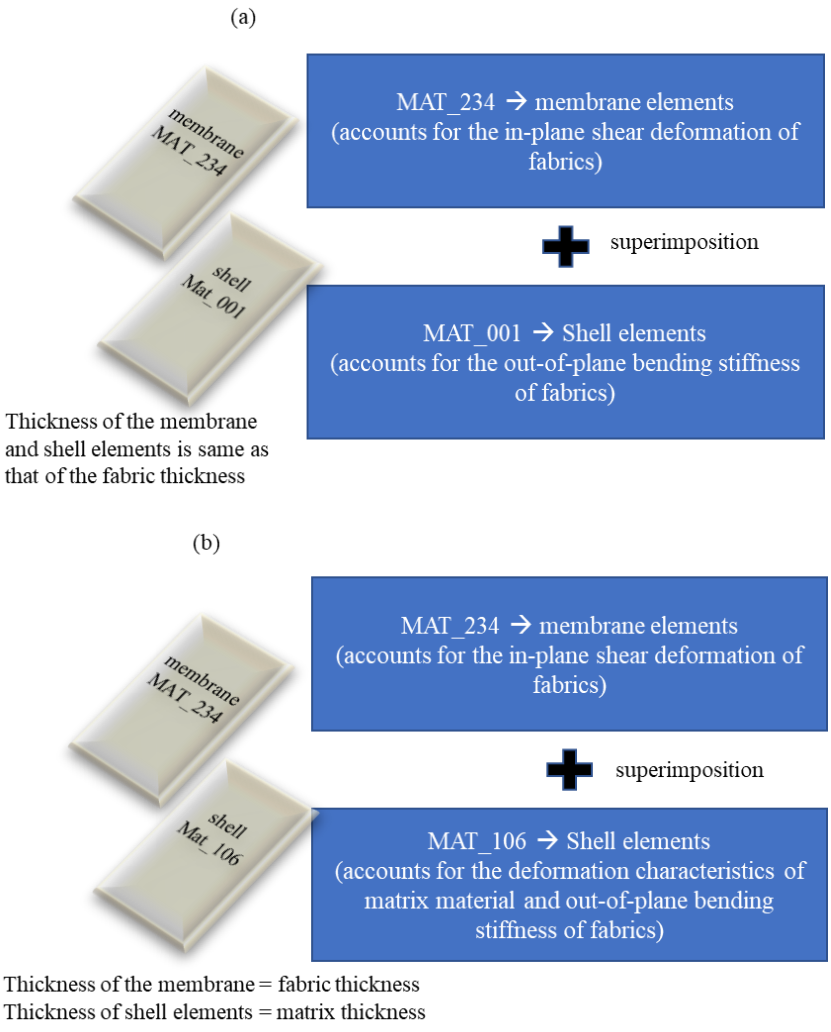

Figure 6: Superimposed approach: (a) dry fabric, (b) fabric-reinforced polymer.

5. RESULTS

Press forming simulations of E-glass fabric/PP prepregs were carried out at different forming temperatures, and the results were compared with the press forming of the single layer of PP. The thickness of the PP layer in the prepreg is the same as the thickness of the single layer of unfilled PP. The draw depth attained in press forming of both materials and the failure locations are presented in this section.

5.1 Effect of forming temperature

The effect of forming temperature on the draw depth of single layer PP and Fabric_3733/PP prepreg at different forming temperatures 25, 75, 100, 125, and 150°C is presented in Table 3. The punch corner radius was 15 mm, and the blank holder force was 800 N. It can be observed in this table that the draw depth for both single layer PP and Fabric-3733/PP prepreg increased with increasing forming temperature, primarily due to the increase in the failure strain of PP. However, the draw depth attained with Fabric_3733/PP is much lower at all five forming temperatures. Forming simulations were also carried out with Fabric_1610/PP and Fabric_1522/PP prepregs at 125°C. The draw depths of all three prepregs are very similar, which means that the difference in the aerial densities of the three fabrics did not influence the draw depth of the prepreg.

Table 3: Draw depth attained at various forming temperatures for a blank thickness of 1 mm and a blank holder force of 800 N (punch corner radius = 15 mm).

		Prepreg		
	Single layer unfilled PP	Fabric_3733/PP	Fabric_1610/PP	Fabric_1522/PP
25°C	19.10	17.02	*	*
75°C	23.11	19.03	*	*
100°C	26.63	19.54	*	*
125°C	29.15	20.03	20.09	20.14
150°C	30.00 (failure in cup wall)	20.04	*	*

From Table 3, it can be seen that the draw depth attained for press forming of a single layer PP just before failure increases with increasing forming temperature, while for the superimposed model of fabric and PP, the draw depth attained before failure does not show any major variation. Failure in the single layer PP was observed at the die entry radius as shown in Figure 7(a) for all temperatures except at 150°C for which failure was observed along the cup wall. At 25°C, failure can be attributed to wrinkling along the flange area, and for 75, 100, and 125°C, failure was observed when the effective plastic strain at the top corner radius exceeded the failure strain of polypropylene.

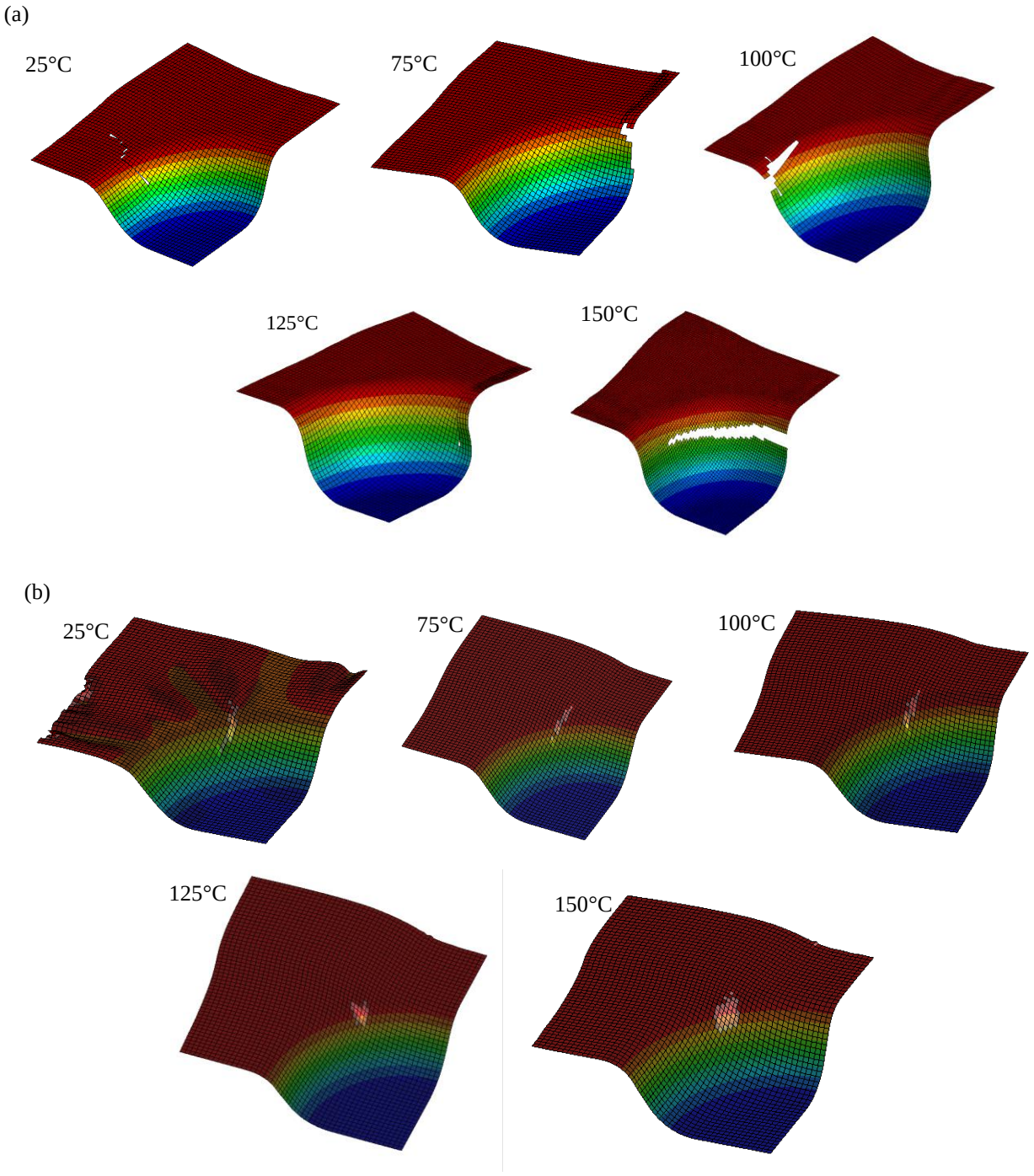

Figure 7: Failure locations of the press formed (a) unfilled PP and (b) fabric-reinforced PP cups at different forming temperatures.

The draw depth attained just before failure during press forming of fabric-reinforced PP prepreg (Figure 7(b)) did not show much variation as can be seen from Table 3. Failure was observed in the PP layer when the plastic strain exceeded the failure strain of polypropylene. The failure in the PP was at the same location as where the maximum shear deformation occurs in the fabric layer (along the diagonal at the die entry

radius). The shear deformation in the fabric layer introduces additional stress in the PP layer which increase the plastic strain at that particular location and ultimately results in the failure of the PP layer.

The small difference in the draw depth for drawn prepreg cups can be attributed to the difference in the failure strain of PP at different temperatures, which increases with increasing temperature. Failure in all prepreg cups was observed at the top corner radius where the shear deformation is maximum in the fabric layer irrespective of temperature or the fabric type. The small difference in the draw depth attained before failure for fabrics with different areal density can be attributed to the small difference in their shear locking angles. The wrinkles that are formed due to shear locking are shape-dependent and process parameters independent [14], and hence the reason for almost the same draw depth for fabric-reinforced PP irrespective of temperature or fabric type.

5.2 Effect of punch corner radius

Table 4 gives the draw depths attained before failure for single layer PP and Fabric_3733 reinforced PP prepreg sheet, each with 1 mm thickness for press forming with 8 mm and 15 mm punch corner radius. The blank holder force was 800 N.

Table 4: Draw depth attained at various forming temperatures for a blank thickness of 1 mm and a blank holder force of 800 N (punch corner radius = 8 and 15 mm).

Forming Temperature	Punch Corner Radius	Draw depth (mm)	
		Single layer unfilled PP	Fabric_3733/PP Prepreg
100°C	8 mm	22.03	16.04
125°C		26.50	16.08
100°C	15 mm	26.63	19.11
125°C		29.15	19.63

Table 4 shows that the draw depth attained before failure using the single layer unfilled PP showed a decrease in their values compared to the draw depth attained with 15 mm punch corner radius, indicating that with the decrease in the punch corner radius the draw depth attained just before failure decreases. For E-glass fabric-reinforced PP drawn cups, the draw depth was also found to decrease with the decrease in the punch corner radius. However, at same punch corner radius the draw depth attained before failure was observed to be same irrespective of the blank temperature. Similar to the press forming with 15 mm punch corner radius, the failure was observed when the shear deformation in the drawn cup reaches shear locking angle in the fabric layer which created additional stresses in the PP layer and when the plastic strain in the PP exceeds the failure strain it causes failure in that particular leading to the failure of the E-glass fabric reinforced PP. After the failure of PP, buckling was observed in the fabric layer leading to ultimate failure of the composite.

Failure locations for the drawn cup with single-layer unfilled PP and the superimposed model of fabric-reinforced PP are shown in Figures 8 and 9, respectively. In all the cases for press forming of E-glass fabric reinforced PP, failure was observed in the PP at the same location where the maximum shear deformation was observed for the fabric layer. When the plastic strain in the PP exceeds the failure strain, the element gets deleted which causes buckling in the fabric layer. Figure 10 shows the individual layer of the PP matrix and the fabric layers just after failure. Buckling in the fabric layers occurs at the same location where the failure occurs in the PP matrix layer.

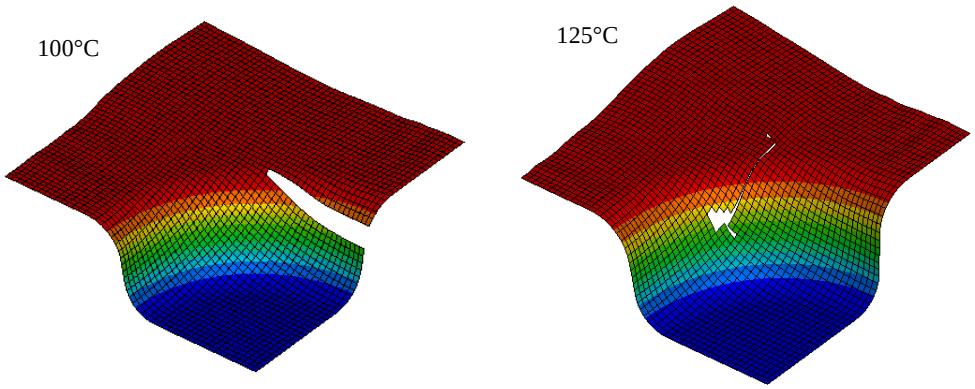

Figure 8: Failure location of the deep drawn unfilled PP cups at different temperatures using a punch corner radius of 8 mm.

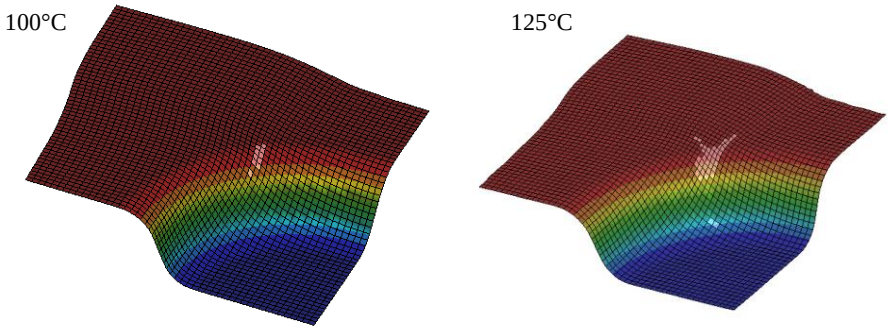

Figure 9: Failure location of the deep drawn Fabric_3733/PP prepreg cups at different temperatures using a punch corner radius of 8 mm.

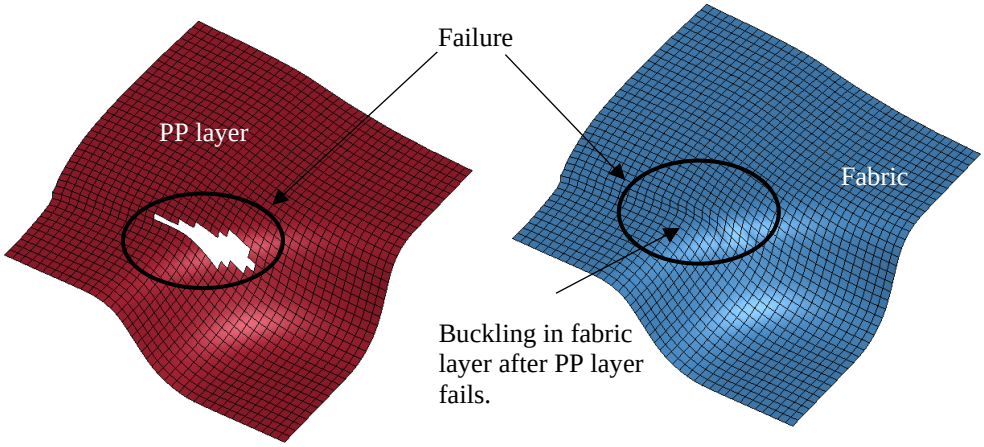

Figure 10: Failure location in the individual layers of fabric and PP for press forming of fabric-reinforced PP.

6. CONCLUSIONS

This study presents a numerical modeling approach for press forming fabric reinforced polypropylene prepregs. The method utilizes a superimposed model in which the fabric is represented by a combination of shell and membrane elements that are overlaid and share common nodes. The membrane elements account for the in-plane shear deformation of the fabric, while the shell elements account for the out-of-plane bending deformation of the fabric and the deformation of the matrix during press forming.

Press forming simulations of the fabric-reinforced PP using the superimposed model shows that during press forming, both the fabric and PP layers deform together. Shear deformation in the fabric layer introduces additional stresses in the PP layer and when the plastic strain in the PP layer exceeds the failure strain of polypropylene, failure occurs in the PP layer which is followed by the buckling in the fabric layer. The maximum shear deformation was observed along the diagonal at the die entry radius and the same was the location of failure observed in the PP layer. The fabric layer exhibits a buckling tendency after failure is initiated in the PP layer at the same location where the maximum shear deformation in the fabric was observed.

Press forming with single PP shows an increase in draw depth with an increase in the forming temperature, while the fabric-reinforced PP failed at almost similar draw depths irrespective of the forming temperature with the first failure observed in the PP layer followed by the buckling in the fabric layer. With increase in the punch corner radius, both the single PP and the fabric-reinforced PP showed an increase in the draw depth attained just before failure. The fabric-reinforced PP did not show much variation in the draw depth with the areal density of the fabrics which can be attributed to the small difference in the shear locking angle of the fabrics.

References

[1] P. Mallick, Processing of Polymer Matrix Composites, Boca Raton, FL: CRC Press, Taylor & Francis Group, 2018.

[2] P. Boisse, N. Hamila, E. Vidal-Salle and F. Dumont, "Simulation of wrinkling during textile composite reinforcement forming. Influence of tensile, in-plane shear and bending stiffnesses," *Composites Science and Technology,* vol. 71, no. 5, pp. 683-692, 2011.

[3] N. Hamila, P. Boisse , F. Sabourin and M. Brunet, "A semi-discrete shell finite element for textile composite reinforcement forming simulation," *Int J Numer Methods Eng,* vol. 79, pp. 1443-1466, 2009.

[4] T. A. Osswald and G. Menges 1923, Materials Science of Polymers for Engineers. (2nd ed.), Munich; Cininnati: Hanser Publishers, 2009.

[5] A. Tabiei and R. Murugesan, "Thermal structural forming simulation of carbon and glass fiber reinforced plastics composites," *International Journal of Composite Materials,* vol. 5, no. 6, pp. 182-194, 2015.

[6] Q. Chen, P. Boisse, C. H. Park, A. Saouab and J. Breard, "Intra/inter-ply shear behaviors of continuous fiber reinforced thermoplastic composites in thermoforming processes," *Composite Structures,* vol. 93, pp. 1692-1703, 2011.

[7] P. wang, N. Hamila and P. Boisse, "Thermoforming simulation of multilayer composites with continuous fibers and thermoplastic matrix," *Composites: Part B,* vol. 52, pp. 127-136, 2013.

[8] M. Nishi, T. Kaburagi, M. Kurose, T. Hirashima and T. Kurasiki, "Forming simulation of thermoplastic pre-impregnated textile composite," *Internation journal of materials and textile engineering,* vol. 8, no. 8, pp. 779-787, 2014.

[9] M. Nishi and T. Hirashima, "Approach for dry textile composite forming simulation," *19th International Conference on Composite Materials,* pp. 7486-7493, 2013.

[10] Y. Zhou and P. K. Mallick, "Effects of temperature and strain rate on the tensile behavior of unfilled and talc-filled polypropylene. Part I: Experiments," *Polymer Engineering and Science,* vol. 42, no. 12, pp. 2449-2460, 2002.

[11] C. K. R. Emani and P. K. Mallick , "A numerical study on warm deep drawing of polypropylene," *Polymer Engineering & Science,* 2023.

[12] C. K. R. Emani, "Press Forming and Formability of Polypropylene, Dry Fabrics and Fabric-Reinforced Polypropylene," Ph.D. Dissertation, University of Michigan - Dearborn, 2022.

[13] "https://www.fibreglast.com/category/Fiberglass_Fabric," Fiberglast, [Online]. Available: https://www.fibreglast.com/category/Fiberglass_Fabric. [Accessed 05 March 2022].

[14] C. K. R. Emani and P. K. Mallick , "Development of forming limit diagrams for dry fabrics," in *Proceedings of the SPE- Automotive Composites Conference & Exhibition,* Novi, Michigan, September 7-9, 2022.

[15] C. I. Chung, W. J. Hennessey and M. H. Tusim, "Frictional behavior of solid polymers on a metal surface at processing conditions," *Polymer Engineering and Science,* vol. 17, no. 1, pp. 9-20, 1977.

[16] J. G. Kaufman, Fire resistance of aluminum and aluminum alloys and measuring the effects of fire exposure on the properties of aluminum alloys, Materials Park, OH: ASM International, 2016.

[17] T. A. Osswald and G. Menges, "4. Thermal Properties of Polymers," in *Material Science of Polymers for Engineers,* Munich; Cincinnati, Hanser Publishers, 2012, pp. 83-110.

[18] S.-J. Park and M.-K. Seo, "Chapter 6 - Element and processing," in *Interface Science and Technology,* vol. 18, 2011, pp. 431-499.

[19] H. Yildirim and F. Ozturk, "A benchmark study of the material models for forming simulation of woven fabrics," *The Journal of the Textile Institute,* vol. 113, no. 6, pp. 1027-1038, 2021.

[20] I. Ivanov and A. Tabiei, "Loosely woven fabric model with viscoelastic crimped fibers for ballastic impact simulations," *International Journal for Numerical Methods in Engineering,* vol. 61, no. 10, pp. 1565-1583, 2004.

[21] N. Hamila and P. Boisse, "Locking in simulation of composite reinforcement deformation. Analysis and treatment," *Composite. Part A, Applied science and Manufacturing,* vol. 53, pp. 109-117, 2013.

[22] R. Azzouz, S. Allaoui and R. Moulart, "Composite preforming defects: a review and a classification," *International Journal of Material Forming,* vol. 14, no. 6, pp. 1259-1278, 2021.

[23] D. Jauffres, J. A. Sherwood, C. D. Morris and J. Chen, "Discrete mesoscopic modeling for the simulation of woven-fabric reinforcement forming," *Internation Journal of Material Forming*, vol. 3, no. 2, pp. 1205-1216, 2010.

[24] P. Harrison, "Modelling the forming mechanics of engineering fabrics using a mutually constrained pantographic beam and membrane mesh," *Composites Part A: Applied Science and Manufacturing*, vol. 81, pp. 145-157, 2016.

[25] B. Tomastrom, "Chapter 2 Thermoplastic composite sheet forming: Materials and manufacturing techniques," *Composite Materials Series*, vol. 11, pp. 27-73, 1997.

[26] C. K. R. Emani and P. K. Mallick, "Effect of shear-tension coupling on the deformation characteristics of woven fabrics," in *Proceedings of the American Society for Composites-37th Technical Conference*, Tuscon, Arizona, September 19-21, 2022.

[27] "LS-Dyna Keyword User's Manual Volume II R11.0," Livermore Software Technology Corporation (LSTC), 2018.